# Sensitivity of Headland Bypassing to Variations in Local Wave Conditions and Regional Climate Drivers.

**D.M. Wishaw[1,2], M.P Barnes[2], J.X. Leon[1], T.R. Mortlock[3], and G. Vieira da Silva[4]**

[1]Univesity of the Sunshine Coast, School of Science, Technology and Engineering

[2]BMT Commercial.

[3]Climate Change Research Centre, University of NSW, Kensington, NSW, Australia.

[4]Griffith University, Coastal and Marine Research Centre.

Corresponding author: Daniel Wishaw (daniel.wishaw@research.usc.edu.au)

**Key Points:**

- Headland bypassing is sensitive to changes in wave direction and height.
- Seasonality was the most significant climate condition that influenced headland bypassing.
- Two modes of headland bypassing are described.

## Abstract

Headland sediment transport is dynamic and complex, but understanding the transport mechanisms is necessary for effective long-term management of downdrift beach compartments. In this study, we have develop a coastal process model using TUFLOWFV, that is used to calibrate an approximation tool for headland bypassing at the study site. The approximation tool is shown to reproduce sediment transport rates at the headland apexes accurately and efficiently. We have explored the headland sediment transport mechanism, the influence of wave height and direction, and the sensitivity in regional climate conditions. Headland sediment transport is shown to occur as 'trickle' bypassing under modal wave conditions or 'sand slug' migration under storm wave conditions that travel in either a headland-attached and a cross-embayment pathway. Bypassing during storm wave conditions produces 50% to 60% of total bypassing volume, despite only accounting for 6% of the recorded days. The results indicate that headland transport is sensitive to changes in wave direction and wave height, with the existing mean wave direction balancing sediment transport on the east and north faces of the headland. Seasonality is the most significant climatic control on headland transport, while ENSO phase is only significant for the headland apexes that are exposed to south-east wave conditions. The potential for anticlockwise rotation of the wave climate in future is explored, with greater erosion of the northern beaches of the headland likely due to a reduced supply of sediment around the eastern point of the headland and greater erosive wave power on the north side.



## Plain Language Summary

We investigated sand movement around a headland, and how it is impacted by waves of different sizes and from different directions. We used Noosa Headland, Australia as our study site, as sand moving around this headland is important for the beach condition of the famous Noosa Main Beach. For average wave size days, we found a slow trickle of sand moves around the headland, however, during larger storm wave conditions, sand was transported in large 'slugs' of sand. Regional climate variability, such as El Niño/La Niña cycles, had little impact on the movement of sand around the headland, while the specific wave height and direction of each storm was important. Southeast waves produced the strongest transport on the east side of the headland, but weak transport on the north side, while northeast waves were the opposite. We found that the existing average wave direction produced balanced transport around the headland, while projected future wave conditions are likely to produce unbalanced transport, with more erosion and less sand arriving on the northern side of the headland. This change will impact Noosa Main Beach, where this pattern is likely to lead to sand starvation of this beach in future years.


## 1. Introduction

Headlands often force a complex hydrodynamic response to wave, wind and tidal conditions that can make prediction of sediment transport around headlands (headland bypassing) difficult to reliably forecast (King et al., 2021; Vieira da Silva et al., 2018). Research relating to headland bypassing is rapidly expanding (Klein et al., 2020) as more tools become available to coastal researchers such as high quality and frequent aerial or satellite images (Wishaw et al., 2021), easier bathymetric survey collection (Silva et al., 2021) and numerical modelling tools (King et al., 2021; McCarroll et al., 2021; Vieira da Silva et al., 2021; Vieira da Silva et al., 2018). Attempts to parametrize headland bypassing using topographical, bathymetric and sediment parameters have been made, however, the interaction between these features and the forcing wave, wind and tidal conditions results in highly localized results that requires specific investigation, particularly at more complex headlands that are substantially different than those used for the parameterization (George et al., 2015; McCarroll et al., 2021).

The regional climate drivers that produce local wind and wave conditions are constantly evolving due to both sub-seasonal to decadal climate variability and climate-change-derived long-term influences (Mortlock and Goodwin, 2015; Mortlock and Goodwin, 2016). Global changes to the wave climate due to global warming include increased wave power, by 0.4% per year (Reguero et al., 2019), robust changes in annual mean significant wave height and mean wave period of 5–15% and shifts in mean deep-water wave direction of 5–15° by the end of the century (Morim et al., 2019). Changes of this magnitude have been shown to influence longshore transport and headland bypassing rates (Splinter et al., 2012; Vieira da Silva et al., 2021), and is expected where headlands are sensitive to wave direction for bypassing or where bypassing requires sequencing of wave conditions to occur for successful headland bypassing (Wishaw et al., 2021). Further research is required to understand the magnitude of this change on headland bypassing at a local scale and its influence on downdrift beaches, which are often highly desirable beach destinations due to the protection of the headland (Wishaw et al., 2020).

To understand local coastal processes and how they may evolve under changing climatic conditions, a range of process based numerical modelling techniques and tools are available (Deltares, 2022),(BMT Commercial Australia, 2022)). However, due to the computational intensity of these models, they are often prohibitive to use for long term simulations. Solutions to this include various schematisation of the wave climate to reduce the number of wave conditions that need to be resolved (Benedet et al., 2016) and the use of process based models to calibrate more simplistic estimates of sediment transport (Barnes, 2015). Regardless of approach, it is important that coastal managers and planners have tools that are both flexible and accurate such that they can be applied to both shorter-term timeframes (weeks-month) and longer-term time frames (years-decades) to help guide management and planning decisions (Splinter and Coco, 2021).

In this study calibrated/validated process-based hydrodynamic, wave and coastal sediment transport models are used to support the development of an efficient headland bypassing approximation tool. This tool is then used to assess the sensitivity of headland bypassing to changes in the regional wave conditions associated with plausible future climate scenarios. The study outputs provide new insights to local headland bypassing that influences the available sediment supply to the downdrift beaches noted for their high social, recreational and economic value. The tool also provides a framework for short-, medium- and long-term forecasts of sediment supply which can be used to support local coastal management decision making and investment.

## 2. Study Area

The study location was at Noosa Headland, in Queensland, Australia (**Figure 1**). Noosa Headland is a medium sized, acute headland with a balanced bathymetric expression (George et al., 2015) that has been used as a study site for previous work (Wishaw et al., 2021; Wishaw et al., 2020). The open coast shoreline is wave-dominated and micro-tidal (Harris et al., 2002). The headland contains several small, embayed beaches, with the eastern facing beach compartments exposed to the dominate modal wave climate and northern facing beaches sheltered from the modal wave conditions, but exposed to east and northeast wave emanating from tropical lows and (ex) tropical cyclones in the Coral Sea.

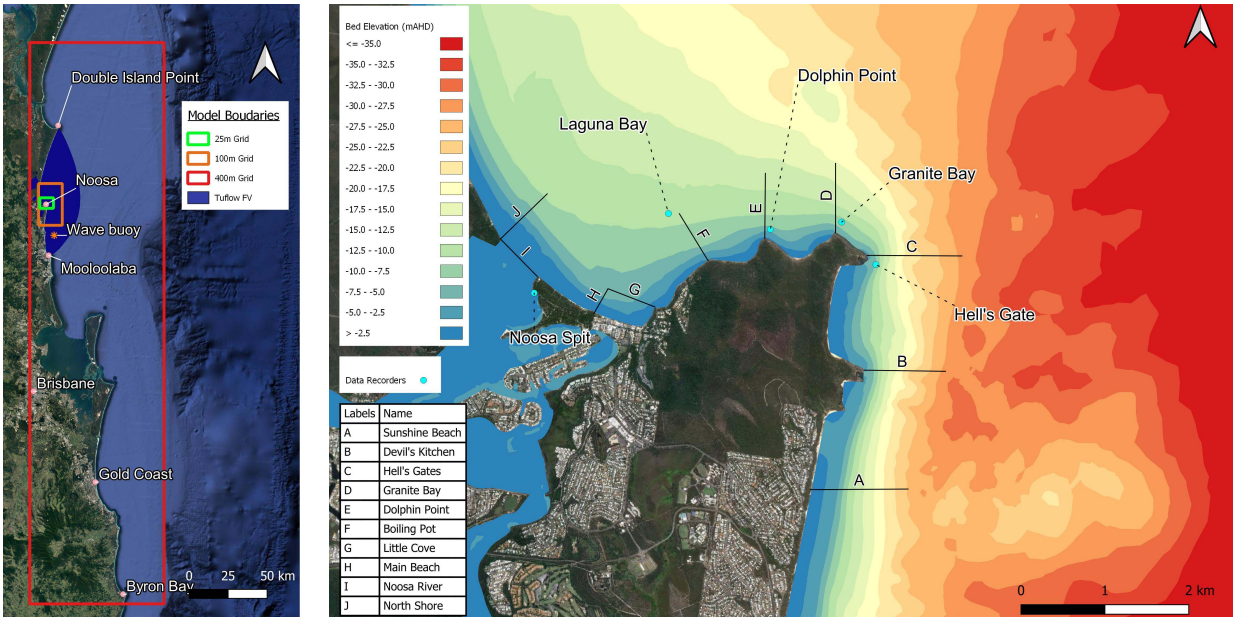


**Figure 1:** Noosa regional setting with the (a) nested model boundaries shown and (b) the nearshore bathymetry and headland apexes labeled.

Wave seasonality at the Mooloolaba wave buoy is defined by larger waves from the east in summer and smaller waves from the southeast in winter (**Figure 2**) (Barnes et al., 2013). Sites further south show a stronger trend of winter swell, including waves from the south-southeast direction (Mortlock and Goodwin, 2015), however at Mooloolaba, protection from Mulgumpin (Moreton Island) and the change in shoreline orientation of the Southern

Queensland coast (regionally orientated at 353 degrees true north) compared with the New South Wales coast (regionally orientated at 12 degrees true north) reduces the exposure to these conditions. Furthermore, the site may be is also annually exposed to cyclonic wave conditions during the summer originating in the Coral Sea (Wishaw et al., 2020) which results in increased wave heights and an anti-clockwise rotation of the wave climate in summer.

Large wave events (Hs>2.5m) can occur at the site from both tropical and extra-tropical storm systems, with tropical systems having a shore normal propagation (easterly) along the coast while extra-tropical storms produce a shoreline-oblique (southeasterly) propagation (Goodwin et al., 2016). Southeasterly wave conditions tend to drive sediment transport north along the coastline in the southern extent of the study area, but are generally protected from influencing the bay beaches on the north side of the headland. In contrast, easterly waves have less impact on long shore transport on the southern beaches, but drive transport through the bay beaches on the north side of the headland (Wishaw et al., 2021). Outside of these storm conditions, the modal wave climate along the east coast of Australia is dominated by a range of synoptic patterns forming in the Coral Sea, Tasman Sea and Southern Ocean that are modulated by the location of the sub-tropical ridge (Mortlock and Goodwin, 2015).

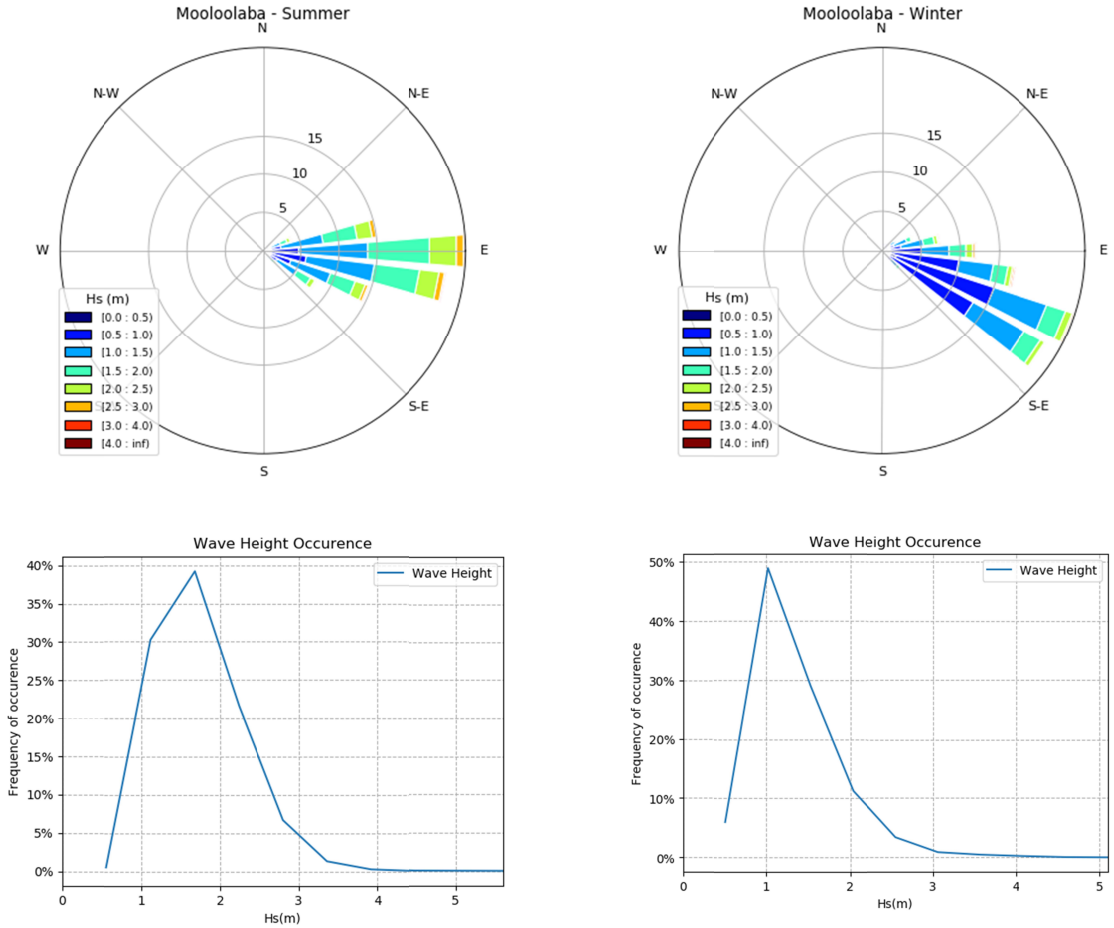


**Figure 2**: Recorded wave conditions for the austral summer (a) and austral winter (b) and wave exceedance for austral summer (c) and austral winter (d).

## 2.1 Conceptual understanding of bypassing at Noosa Headland

Previous research at this site undertook a shoreline change analysis using 60-years of aerial imagery in conjunction with local directional wave data to develop a preliminary understanding of the mechanism of headland bypassing (Wishaw et al., 2021). This assessment concluded that episodic headland bypassing was linked to a specific

sequence of wave conditions with waves larger than $H_s$ = 2.5m from the southeast being followed by waves larger than $H_s$ = 2.5m from the east-northeast. Furthermore, the calculated annual sediment budget (-8,900$m^3$/year) of the protected Noosa Main Beach, indicates that it is currently experiencing significant erosion stress, with increased erosion predicted under future climate conditions. Finally, this previous work evaluated the correlation between ENSO phasing and beach widths, with exposed eastern beaches having a negative correlation with ENSO phase, while the protected beaches on the north of the headland did not show a significant correlation, due to the reliance of the episodic bypassing.

# 3. Process-based modelling

## 3.1 Model development

A SWAN (wave) and TUFLOW FV (coastal hydrodynamics and sediment transport) model combination was used to simulate the coastal processes at Noosa Headland (**Figure 1**). SWAN is a third-generation phase-averaged wave model based on fully spectral representation of the action balance equation, accounting for wave-current interaction through radiation stress, refraction, wind generation, whitecapping, nonlinear wave-wave interactions, bottom dissipation, and depth-induced breaking (Delft University of Technology, 2016). The SWAN model for the study area was previously developed and calibrated (Wishaw et al., 2020), and comprises the system of nested grids shown in **Figure 1**. Waves in the nearshore areas around Noosa Headland are resolved at 25m resolution (from the shoreline to approximately 35m depth), with the deeper water conditions sufficiently captured at lower resolution. using three nested grids that step down from a 400m grid that extends to the continental shelf, a 100m regional grid and a 25m grid in the study area. The nested wave models utilize water level outputs from the hydrodynamic model that are passed through to SWAN from TUFLOW FV after simulating tide, wind, and mean sea level pressure to ensure accuracy of the wave interaction with the seabed in shallow water.

TUFLOW FV is a flexible mesh finite volume numerical model that solves the conservative integral form of the nonlinear shallow water equations to simulate hydrodynamics, sediment transport and water quality processes in 3d or in a depth averaged 2d and 1d modes (BMT Commercial Australia, 2022). For this research, hydrodynamics and sediment transport modules were utilized in a depth averaged 2d configuration . The model mesh resolution varies from 1900m grid at the offshore boundary grid that was downscaled to a ~50m grid in the nearshore area of interest (where higher rates of sediment transport are typically observed). The model mesh resolution smoothly downscales using triangular and quadrilateral cells.

Bathymetry inputs for the model utilized the same combination of inputs as per the SWAN model, which are defined through a combination of the flowing datasets: i) a 2m resolution Digital Elevation Model (DEM) created from a hydrographic survey of the lower Noosa river and parts of Laguna Bay; ii) , a 2011 bathymetric LiDAR survey of the Sunshine Coast (Queensland Government, 2012)extending from the shoreline to ~20m depth ; iii) and a high-resolution (30m) depth model for the Great Barrier Reef in areas further offshore (Geoscience Australia, 2017).

Spatially and temporally varying wind field and mean sea level pressure inputs are derived from the NOAA CFSR and CFSv2 global model datasets (Saha, 2014; Saha, 2006). The tidal water level variation used to define the hydrodynamic model offshore boundary is based on Mooloolaba Tide gauge recordings (Queensland Government, 2019a) and scaling developed as part of the model calibration process. The wave model offshore boundary (applied at the eastern boundary of the 400m grid) is defined using nonstationary peak wave parameters derived from the Mooloolaba Wave buoy recordings (Queensland Government, 2019b) and deep water wave transformation.

Non-cohesive coastal sediment transport is modelled following (Van Rijn, 2007a; Van Rijn, 2007b; Van Rijn, 2007c) as implemented within TUFLOW FV, allowing simulation of multiple fraction sediment transport including wave- and current-related bedload and suspended load. The presence of waves can enhance sediment pickup and therefore also the rate of transport by the local currents. The prediction of wave-related sediment transport due to processes such as wave velocity skewness and wave boundary layer streaming is also represented. These (and other) processes can generate a net transport in the direction of (or against) wave travel, even in the absence of a local current.

## 3.2 Data collection for model calibration/validation

For calibration of the coastal process model, current data was available from several locations around the headland for a study period that included a range of wave conditions assumed to promote nearshore sediment transport. The coastal process model was developed in two stages, with the wave model originally developed for a previous piece of research (Wishaw et al., 2020) and calibrated using data recorded by a bottom-mounted (approx. 9m depth) acoustic-doppler current profiler (ADCP) in Laguna Bay. An existing hydrodynamics model developed for a project focusing on the Noosa River estuary (Barnes et al., 2019) used water level and current recordings from the same ADCP deployment for model development and calibration purposes. This existing hydrodynamic model domain was retained for the work described herein, however the model mesh was modified with higher resolution added to the nearshore open coast areas of interest. Three Maroette tilt-flow current meters (Marine Geophysics Laboratory, 2022) were deployed around Noosa Headland to further validate the model results in the study area. The tilt-flow current meters were deployed in a shallow water (approximately 8m) near three of the headland apexes (**Figure 1(b)**) from 1/12/2020 where they were able to collect both modal and storm conditions. Failure of the current meters was an issue, with current meters breaking and being lost, although fortunately retrieved from nearby beaches for two of the three current meters, with the Hell's Gate current meter not retrieved.

## 3.3 Model calibration/validation results

Model validation was undertaken for the period 1/12/2020 to 18/12/2020, with the Granite Bay period limited to 15/12/2020 before device failure. The model validation period captured a range of conditions, with smaller modal wave conditions and a strong wave event emanating from a tropical low in the coral sea that produced wave heights with an approximate annual recurrence interval of one year. The validation period was curtailed due to instrument failure; however, the peak of the wave event was captured on retrieved data for both Dolphin Point and Granite Bay sites. However, the model validation period was sufficient to capture a sufficiently representative range of conditions when compared with the total wave climate (**Figure 6**). A full list of the calibration parameters can be found in appendix 1, while the modelling workflow is provided in **Figure 3**: Coastal process model modelling workflow**Figure 3**.

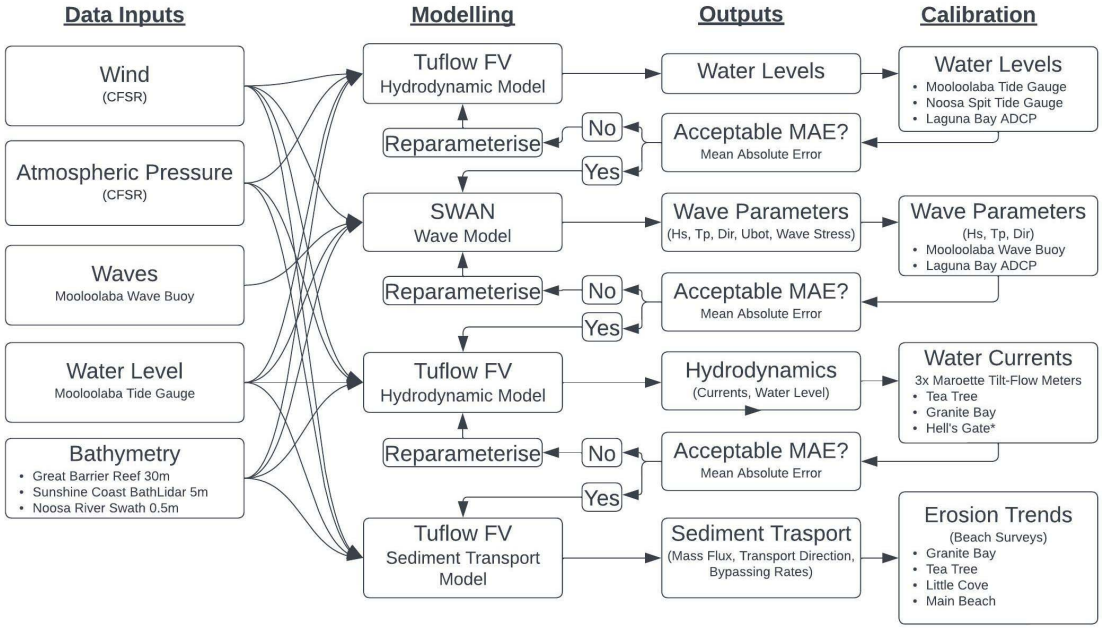


**Figure 3**: Coastal process model modelling workflow

Wave height and direction are provided as well as recorded and (depth-integrated) modelled currents in **Figure 4**. Model skill was assessed by calculating bias, $R^2$ and Mean Absolute Error (MAE), the results of which are displayed

in Table 1. The model shows good skill with reproducing the observed currents, with peak current velocity magnitude and timing generally well produced. Model results from Dolphin Point show that the magnitude of the peak currents on 13/12/2020 and 15/12/2020 were underrepresented, during a period where wave direction rapidly transitions from a southeast direction to a north-northeast direction. Given that the wave input data is only representing the peak wave direction, it is likely that a multi-directional wave climate is influencing the recorded currents but is not being adequately resolved in the modeled data, which has been observed in previous headland bypassing studies (e.g.(Vieira da Silva et al., 2016) that used the full spectrum as boundary conditions. While a multi-modal input, or the full spectrum, such as Wave-Watch 3 could have been used to inform the wave boundary condition, the development of the approximation tool is intended to be implemented using easy to access open-source data, and as such the wave buoy data was used. Despite this limitation, the model is still resolving the currents well with a high $R^2$ and low MAE and Bias for the two locations, with Dolphin Point performing better than Granite Bay, particularly for low current speed conditions. Moreover, under lower current conditions significantly less sediment is transported. Given the limitations of the model design, particularly with a model bathymetry that is derived from a 2011 bathymetric survey, the model results are satisfactory for the purposes of this research.

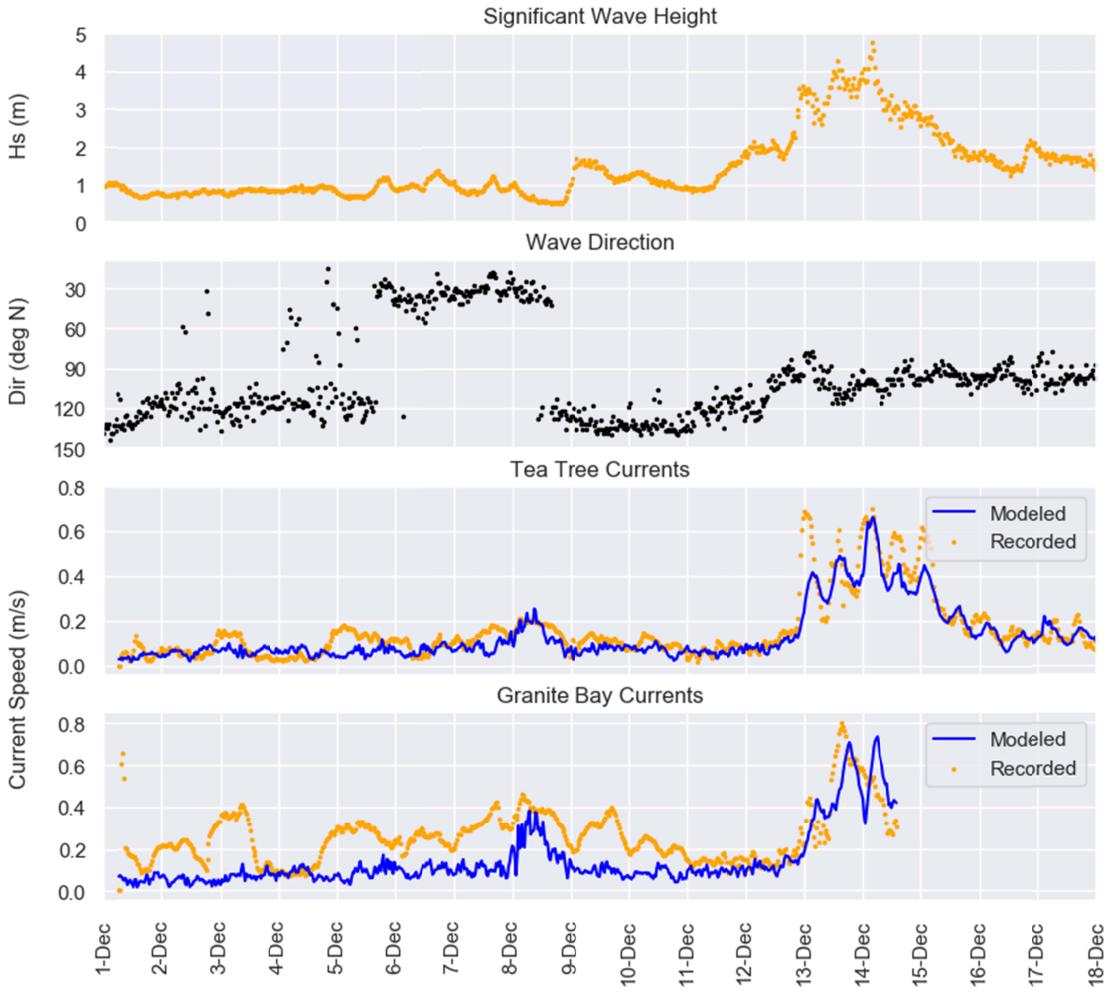


**Figure 4** : Validation data for the period 01/12/2020 to 18/12/2020 with recorded significant wave height (top), wave direction (second top), currents at the Dolphin Point site (third top) and currents at the Granite Bay site (bottom).

Table 1: Model validation statistics for Dolphin Point and Granite Bay locations.

| Location | N | BIAS (m/s) | MAE (m/s) | $R^2$ |
|---|---|---|---|---|
| Dolphin Point | 899 | -0.03 | 0.05 | 0.92 |
| Granite Bay | 684 | -0.12 | 0.14 | 0.71 |

## 3.4 Modelled sediment transport and headland bypassing

Calibration of coastal process models with respect to sediment transport rates is difficult, due to the large spatial area of the model domain, variability of transport rates under different forcing and the challenges in doing field work during events that would be useful to the calibration period. Other studies have utilized a Helley-Smith sampler (Helley and Smith, 1971) to measure bedload transport rates for calibration of the numerical model, which required a substantial investment in equipment and expertise to carry out (Vieira da Silva et al., 2016). Despite this, the Helley-Smith was developed for use in rectilinear flow conditions and is not particularly accurate in complex flow environment as deviations in the angle of flow to the mouth of the sampler can cause recirculation within the instrument and reduce the sampling efficiency, without any plausible way to correct for these current deviations (Gaudet et al., 1994). Consequently, we used survey data that was previously collected (Wishaw et al., 2020) to assess the order of magnitude of sand migration within the coastal compartments between headland apexes to assess the performance of the sediment transport model across the period from 20/02/2019 to 28/02/2019. The results indicate good alignment between the sediment transport model and the observation of erosion and accretion, with higher levels of erosion in the outer compartments and net deposition in the more protected compartments. At Dolphin Point, sediment transport was higher than the survey data would suggest, but a review of the model outputs shows a sediment transport split at this location, with transport remaining attached to the headland and also being deflected north (**Figure 6**).

The process-based model illustrates the sensitivity of the nearshore coastal processes to variation in wave height and direction, particularly around the 2.5m significant wave height threshold previously hypothesized (**Figure 5**). Waves from the southeast set up longshore transport along the exposed coast south of the headland, resulting in bypassing of the easterly orientated headland apexes even at lower wave heights (**Figure 5**a). Larger waves with a south-east orientation produce more energetic bypassing of the eastern points, with sediment freely transported toward the northern apex of the headland, where current velocities decrease behind the headland apex, allowing for sediment deposition, or continue north, becoming detached from the headland completely and transporting sand in a cross-embayment pathway (**Figure 5**d). Smaller waves approaching from the mean wave direction of 95 degrees (east) produce limited transport around the headland (**Figure 5**b), with larger waves creating strong sediment transport conditions along the northern side of the headland (**Figure 5**e). Larger waves with a northeast orientation energise the northern compartments of the headland, but without the strong transport from Hells Gate to Granite Bay seen in the east conditions (**Figure 5**f).

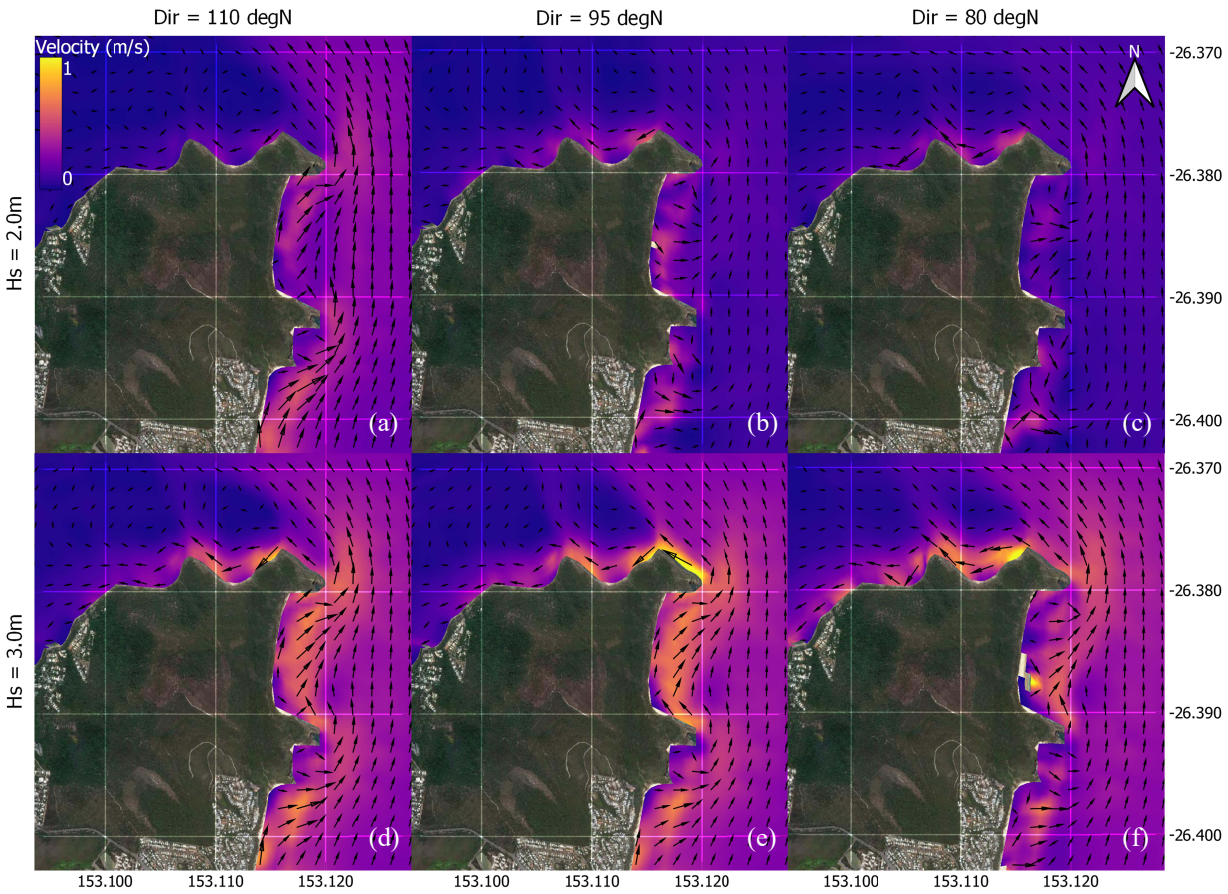


**Figure 5**: Sensitivity of nearshore current velocity to variation in the wave climate.

## 4. Headland Bypassing Approximation Tool

### 4.1 Tool development

While the process model described above was relatively computationally efficient, the use of a process model for time frames longer than a few months becomes impractical from both a computation and data storage and processing requirement. As such, a method of schematization of the model inputs was desirable to assess wave conditions for periods of years to decades. Several methods were reviewed for implementation (Benedet et al., 2016), with methods such as the 'Energy Flux Method' used in other headland transport investigations (Vieira da Silva et al., 2021). For this research, a Fixed Bin approach was taken, whereby available directional wave data was used to describe the wave conditions and the model simulated conditions that bounded observed wave conditions (**Figure 6**). The model simulations were run with bin sizes of 10 degrees and 1m for wave direction and wave height, which were then linearly resampled and interpolated to 1 degree and 0.1 meters respectively. Wave period was also evaluated in an initial test of the tool, with wave period bin sizes of 2 seconds, however, this did not significantly improve the accuracy of the results but did significantly increase the number of required simulations and the complexity of the tool. Consequently, wave period was parameterized by taking an average wave period for each wave height, resulting in a total of 86 bins. While this is significantly higher than the target for the Energy Flux Method, the Fixed Bin approach was preferred as it provided more evenly distributed points that allowed for more accurate interpolation and therefore higher resolution across all possible wave conditions.

A relationship between offshore wave conditions at the Mooloolaba wave buoy and sediment transport at each headland apex (**Figure 1**) was established and loaded into a database to create the Headland Bypassing Approximation Tool (HBAT). The accuracy of the sediment bypassing estimates from the HBAT was calibrated

against a period simulated in the calibrated process-based model, using daily averaged sediment transport volumes. The calibration period was between 01-02-2019 to 31-03-2019 that contained large wave conditions from Tropical Cyclone Oma and overall represented a wide variety of potential wave conditions (**Figure 6**). A calibration factor was applied for each headland apex to ensure a suitable match between the HBAT results and the process-based model results and validated against the period 01-12-2020 and 31-01-2021 which contained a diverse range of wave conditions, including large waves.

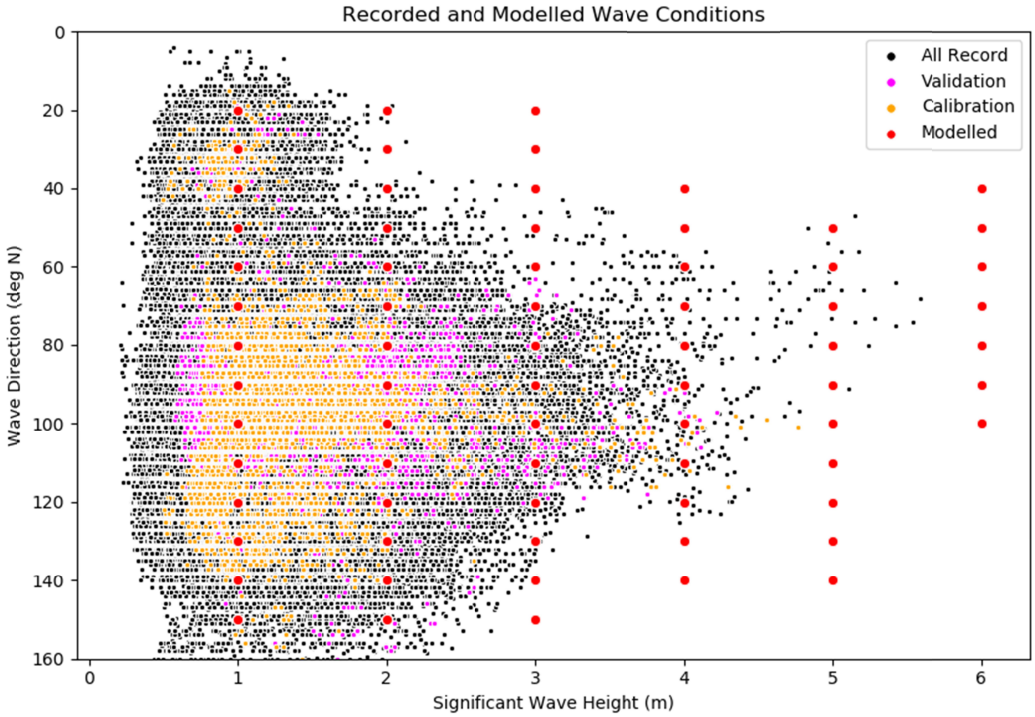


**Figure 6:** Recorded daily wave conditions for all records at the wave buoy (black), for the Tropical Cyclone Oma period (orange), the Tropical Cyclone Oma validation period and modelled wave conditions (red).

## 4.2 Tool validation

Validation of the HBAT was undertaken for a 91-day period from 30/11/2020 to 01/03/2021, aligning, with some extension, with the validation period for the process based model above and including a variety of wave conditions. The results showed excellent skill at reproducing the bypassing volumes from the process-based model (**Figure 8**) with a mean $R^2$ value for each location equal to 0.9. The model uses a simplified wave-period relationship to reduce complexity, although testing of this approach indicated that there was limited impact on the daily bypassing volumes. The validation results indicate a good match between the two datasets, although the model tends to over-estimate bypassing for large conditions at Boiling Pot. The results are overall excellent, especially considering the very significant improvement in computational efficiency compared with the process-based model.

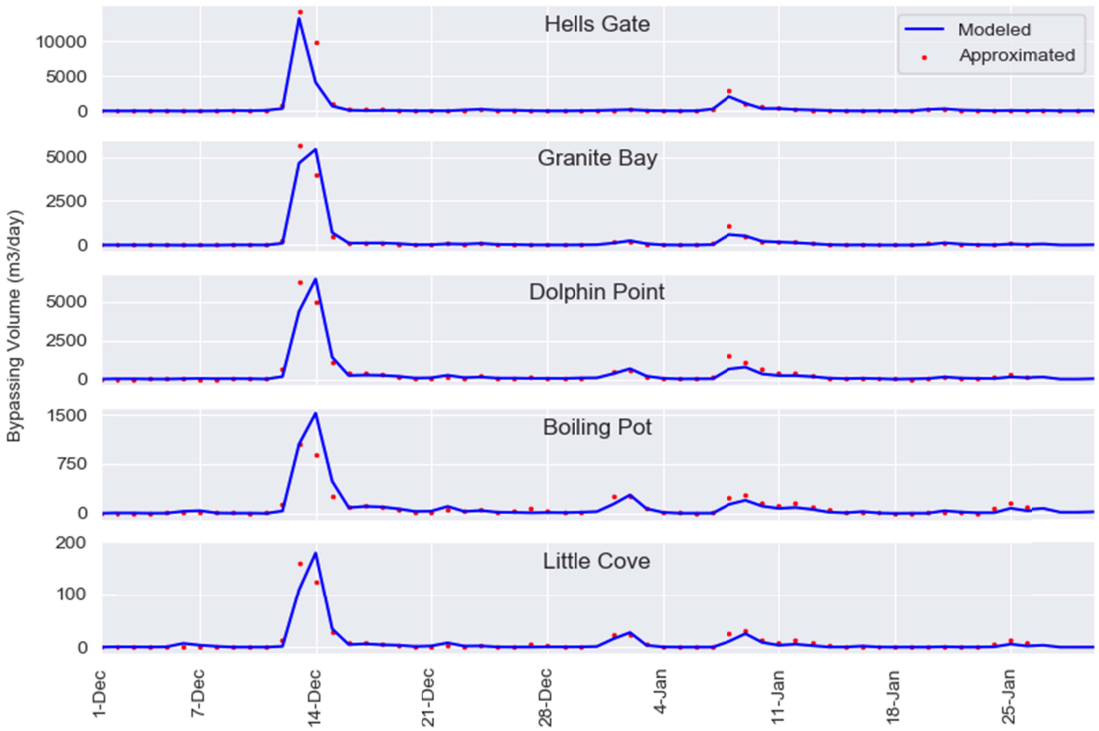


**Figure 7:** Validation of the HBAT against the process-based numerical model. The HBAT (red dots) shows a strong similarity with the process-based model for most conditions, with some underestimation of bypassing at Boiling Pot.

## 5. Headland Bypassing Assessments

### 5.1 Assessment scenarios

Bypassing sensitivity at each of the headland apexes was evaluated for wave parameters (wave height, wave direction) as well as climatic drivers that influence wave formation in the Coral and Tasman Seas. Climatic drivers included the medium-term trends of ENSO phase and seasonality and transient trends derived from the regional synoptic modality including storminess and synoptic type. Each of these variables was assessed using the full recorded period of directional wave data from the Mooloolaba Wave buoy (2006-2022).

Changes in headland bypassing due to changes in wave height and direction were assessed using the HBAT to understand the sensitivity of headland bypassing to changes in these parameters. Within this evaluation, the relative bypassing rates of the headland apexes were evaluated, with particular focus on the long term mean wave direction. A further visual evaluation of the near-shore current set up was undertaken using outputs from the process-based model around the wave height and directions identified in the previous study (Wishaw et al., 2021). The overall wave climate was separated into modal and storm conditions based on the approach of Mortlock and Goodwin (2015), although simplified with respect to storm thresholds. Mortlock and Goodwin assessed the wave threshold values for separation between modal and storm conditions for southeast Australia and concluded that the $Hs_{10}$ value serves as a reasonable approximation of this boundary. Based on the Mooloolaba wave buoy recordings available to this study, the $Hs_{10}$ value is 2.1m for summer and 1.75m for winter. Wave heights above this threshold were defined as ‘storm’ conditions, while wave heights under this threshold were considered ‘modal’ and further grouped. This grouping utilised a k-means clustering algorithm to identify clusters within the Mooloolaba wave data and assess regional synoptic dissimilatry from long term trends.

Several previous studies have identified that changes in inter-annual or multi-decadal climatic indicies can result in changes to shoreline orientation around headland features, as a consequence of changes to headland bypassing

patterns (Goodwin et al., 2013; Mortlock and Goodwin, 2016; Silva et al., 2021). A previous assement of the relationship between ENSO phase and beach width change at the study site (Wishaw et al., 2021) concluded that there was a negative correlation between the SOI value and the change in beach width for east facing beaches, while no trend was discernable on the protected beaches due to episodic bypassing. Since the 2021 publication, a further two summers of strong La Niña conditions have been experienced at the site, which is significant given the directional wave data set only commences in 2006, with only one La Niña phase recorded previously.

For ENSO phase, modality and seasonality, the daily bypassing rates for each headland apex was evaluated across the full period of avialbe data and then compressed to produce an average annual bypassing rate for each condition, as both the prevelance and power of each condition are significant in bypassing.

## 5.2 Synoptic Clustering

Waves impacting the east coast of Australia are generated in a limited number of wave generation zones due to the sheltering of eastern Australia by New Zealand to the east and southeast and several tropical islands to the northeast. These wave generation zones include the Tasman and Coral Seas and a South-Pacific window between New Zealand and the tropical islands (Paula da Silva et al., 2021). Within these wave generation zones, waves are primarily generated by a number of specific synoptic patterns that have been previously described by Mortlock and Goodwin (2015). The work by Mortlock and Goodwin used wave buoys as far north as Brisbane in their evaluation, which we have extended further northward to the Mooloolaba buoy, given the significant sheltering of southerly wave conditions by Mulgumpin (Moreton Island).

To derive the synoptic conditions that generate modal conditions for the study site, an iterative process was adopted using a k-means clustering algorithm and the generation of synoptic difference plots for each derived cluster. The k-means clustering algorithm is a non-hierichical clusstering method that seeks to find the optimal Voroni cells in mulitdimensional datasets for ‘k’ clusters and returns a centroid for each cluster (Dabbura, 2018). The clusters are determined by minimising the sum of dissimilarites between each object and the centroid for the cluster. The minimum dissimilarity will be obtained with ‘k’ equal to the total number of data points (n) (i.e. where each data point is its own cluster), which is not desirable. Techniques such as the ‘elbow’ method can be used to identify ‘k’ numbers that are placed at an inflection in the diminishing returns of dissimilarity between ‘k’ equals 1 and ‘k’ equals ‘n’.

For the Mooloolaba data, the model was trained on significant wave height, peak period and peak wave direction for waves under the storm threshold. Using the ‘elbow’ method, significant inflections were identified between ‘k’ equals 2 and ‘k’ equals 6, with a long tail distribution thereafter. For all varaitions of ‘k’, the groups split on wave direction only, as wave height and and wave period could not sufficiently deliniate independanet clusters, a result that was previously found by Mortlock and Goodwin.

From each of these clusters a synoptic dissimilarity plot was produced and evaluated to determine if there is a suitable synotptic explanation to the wave condition. To do this, synoptic pressure across the area of interest for each day within a cluster is averaged to produce an average synoptic condition for the cluster, which is then subtracted from the mean long-term (1991 to 2020) synoptic pressure to derive the synoptic anomaly (NOAA, 2022). This process was undertaken for each group of clusters between k = 2 and k = 6, with the best results produced where k=3, in line with the results from Mortlock and Goodwin (2015). The final clusters that were derived included tightly grouped eastern and south-eastern clusters with more disperesed and slightly less energetic northeast clusters (**Figure 8**).

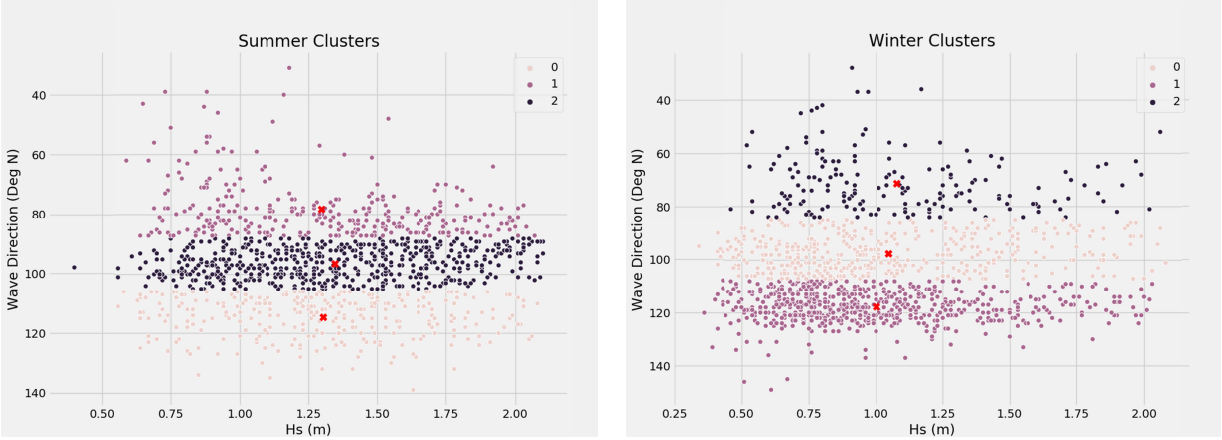


**Figure 8:** Mooloolaba wave buoy derived clusters for both (a) summer and (b) winter.

The clusters (Table 2) produced strong synoptic difference plots (**Figure 9**), with generally stronger synoptic anomalies in the winter than in the summer. Northeast wave conditions are shown to be the result of a low-pressure trough over Eastern Australia and a blocking high pressure over New Zealand. Easterly wave conditions in summer do not show a strong anomaly, suggesting that similarity with the mean long term synoptic state, while in winter a stronger high-pressure anomaly east of New Zealand is present with a weak southern Tasman low pressure anomaly. Southeast wave conditions are produced by a central Tasman Low, zonal circulation pattern with high pressure over southeast Australia and central Pacific. The synoptic anomalies derived for the Mooloolaba site shows strong similarities with other locations along the east coast of Australia (Mortlock and Goodwin, 2015), with a noticeable absence of synoptic patters in the southern ocean that produce southerly wave conditions.

Table 2: Modal cluster statistics

| Season | Mode | Hs Centroid | Dir Centroid | Tp Centroid | Season prevalence |
|---|---|---|---|---|---|
| Summer | Mode 1 | 1.27 | 76.1 | 7.7 | 28% |
| Summer | Mode 2 | 1.31 | 95.1 | 8.9 | 51% |
| Summer | Mode 3 | 1.27 | 113.8 | 9.3 | 21% |
| Winter | Mode 1 | 1 | 71.4 | 7.7 | 14% |
| Winter | Mode 2 | 0.98 | 97.5 | 9.8 | 34% |
| Winter | Mode 3 | 0.95 | 117.7 | 10.6 | 51% |

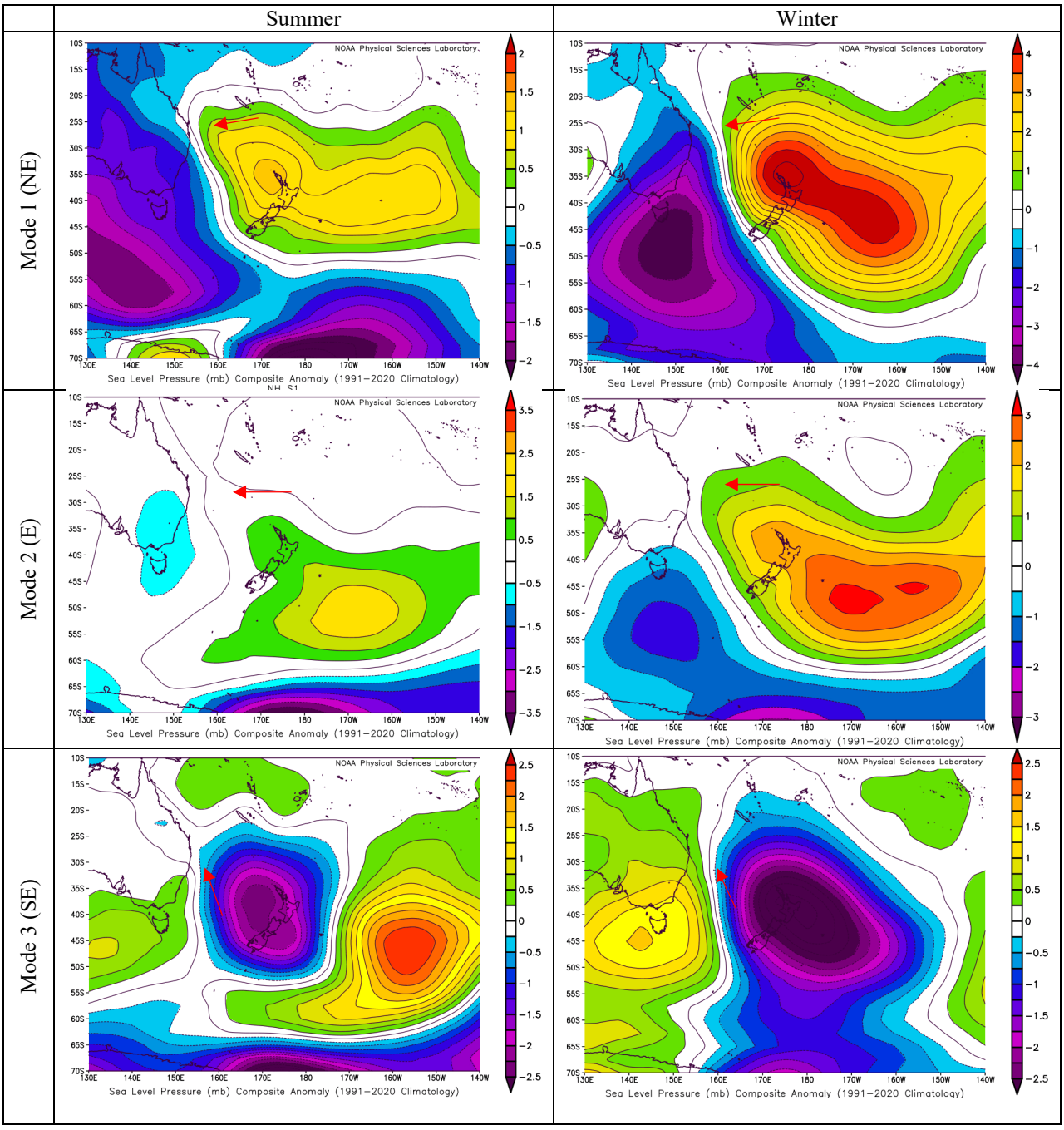


**Figure 9:** Synoptic dissimilarity plots for the derived clusters for the Mooloolaba Wave buoy (NOAA, 2022). These are derived by averaging the synoptic pattern from all days in each cluster and subtracting from the long term average synoptic conditions. Red arrows indicate swell direction from the synoptic anomaly towards the study site.

## 5.3 Headland Bypassing Sensitivity

Headland bypassing rates were shown to be sensitive to both wave direction and wave height (**Figure 10**). Bypassing sensitivity exhibited an exponential increase in sediment transport with wave height, with low bypassing rates when the significant wave height was less than 2m (the typical range of 'modal' conditions). The headland

apex that was orientated to the east (Hell's Gate) showed peak bypassing rates when the wave direction was equal to 120 degrees (southeast), while the north facing points had peak bypassing rates between 70 and 85 degrees (northeast). This range of wave directions is consistent with the boundary of the first standard deviation of wave direction for the site and aligns with the mean wave directions of the clusters described in the previous section. As such, the existing wave climate exists in a 'goldilocks' zone, where both east facing apexes and north facing apexes are efficiently activated to ensure bypassing around the whole headland.

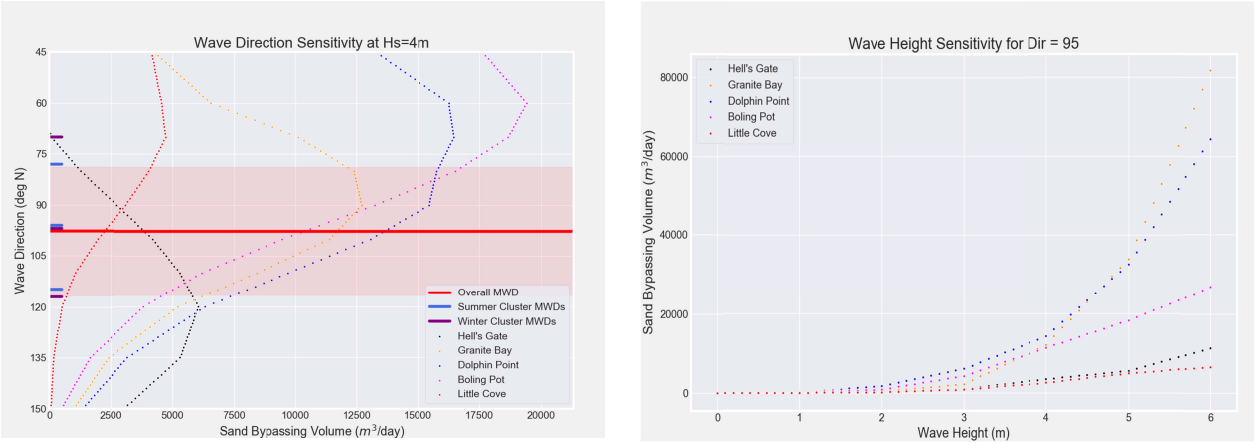


**Figure 10:** Daily bypassing rates at (a) Hs=4m including the mean wave direction with a 1 standard deviation buffer and (b) wave direction = 95 degrees approximately at the mean wave direction.

An assessment of climatic conditions that may modulate the wave conditions was undertaken for seasonality, ENSO phase, modality, and synoptic clusters (**Figure 11**). It is evident that summer is the most active season for headland bypassing, mostly due to the presence of tropical low and tropical cyclones in the Coral Sea that provide east and northeast wave energy. Winter was the weakest season for bypassing at all sites, with autumn and spring transitional between the two extremes.

La Niña conditions exhibited higher bypassing rates than El Niño or ENSO neutral conditions, with the relative increase higher at Hell's Gate, where there is more influence from southeast wave conditions. However, there is a relatively short record of wave conditions compared with the number of El Niño or La Niña events, and strong variability within these samples, with the relationship between ENSO phase and bypassing volume not being statistically significant. Storm conditions (6% of recorded days) provide a larger proportion of the bypassing at the most headland apexes, except for Boiling Pot. The deep seabed at Hell's Gate, Granite Bay and Dolphin Point requires larger waves to initiate transport, while a shallower seabed at Boiling Pot will facilitate greater sensitivity to smaller wave conditions, while combined with the greater prevalence of these conditions (94% of recorded days) results in Boiling Pot being influenced by modal conditions more than storm conditions.

Of the various synoptic patterns derived for Noosa that influence modal wave conditions, the summer clusters dominated for overall sediment bypassing volume at all locations. For both winter and summer, the synoptic conditions that resulted in easterly wave conditions were the most significant, with the northeast sector in summer also significant for the headland apexes on the north side of the headland.

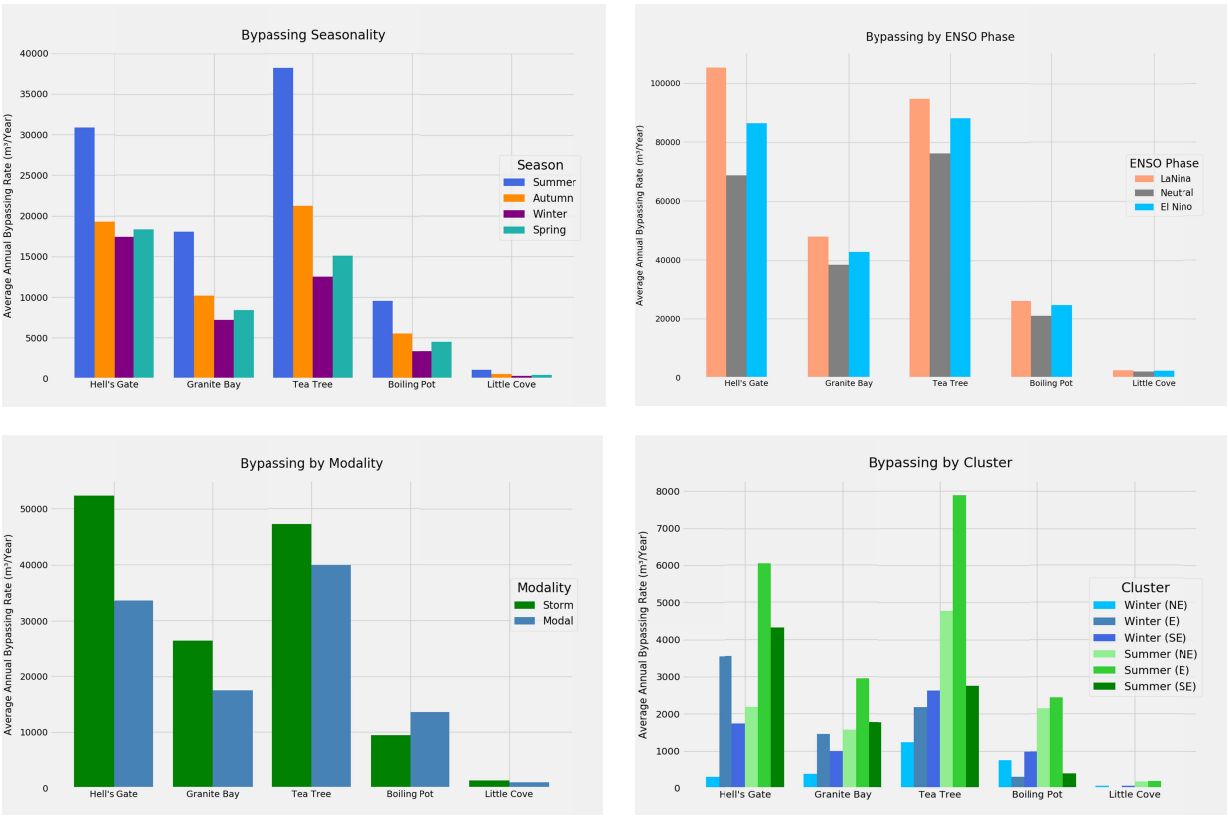


**Figure 11:** Influence of climatic drivers on bypassing rates for all headland apexes at Noosa Headland including (a) seasonality, (b) ENSO phase, (c) modality, and (d) regional synoptic conditions.

## 6. Discussion

Coastal processes around headlands present an interesting challenge for researchers and coastal managers alike, as a detailed comprehension of the coastal processes requires the use of specialist modelling, which is intensive to develop, calibrate and implement, particularly over long study time frames. Nevertheless, the results are critical for understanding the availability of sediment at downdrift beaches. Our results from a Noosa Headland case study show that detailed coastal process models can be developed and used to calibrate an approximation tool that is capable of reproducing headland sediment bypassing rates with a high degree of accuracy, while also capable of being used with readily available datasets and lower technical expertise. This approximation tool has been utilised to investigate an extensive dataset (16 years) of coastal data to develop a better understanding of headland sediment bypassing with respect to wave climate and regional climatic variability.

### 6.1 Headland Bypassing Pathways

Previous research at this site (Wishaw et al., 2021) developed a conceptual understanding of bypassing of the headland, that this research has expanded into a complete understanding of nearshore coastal processes. The previous work hypothesized bypassing to occur under moderate wave forcing via the migration of large ‘sand slugs’, and while this remains valid, a more comprehensive understanding of sediment transport pathways has been illuminated in this research (**Figure 12**).

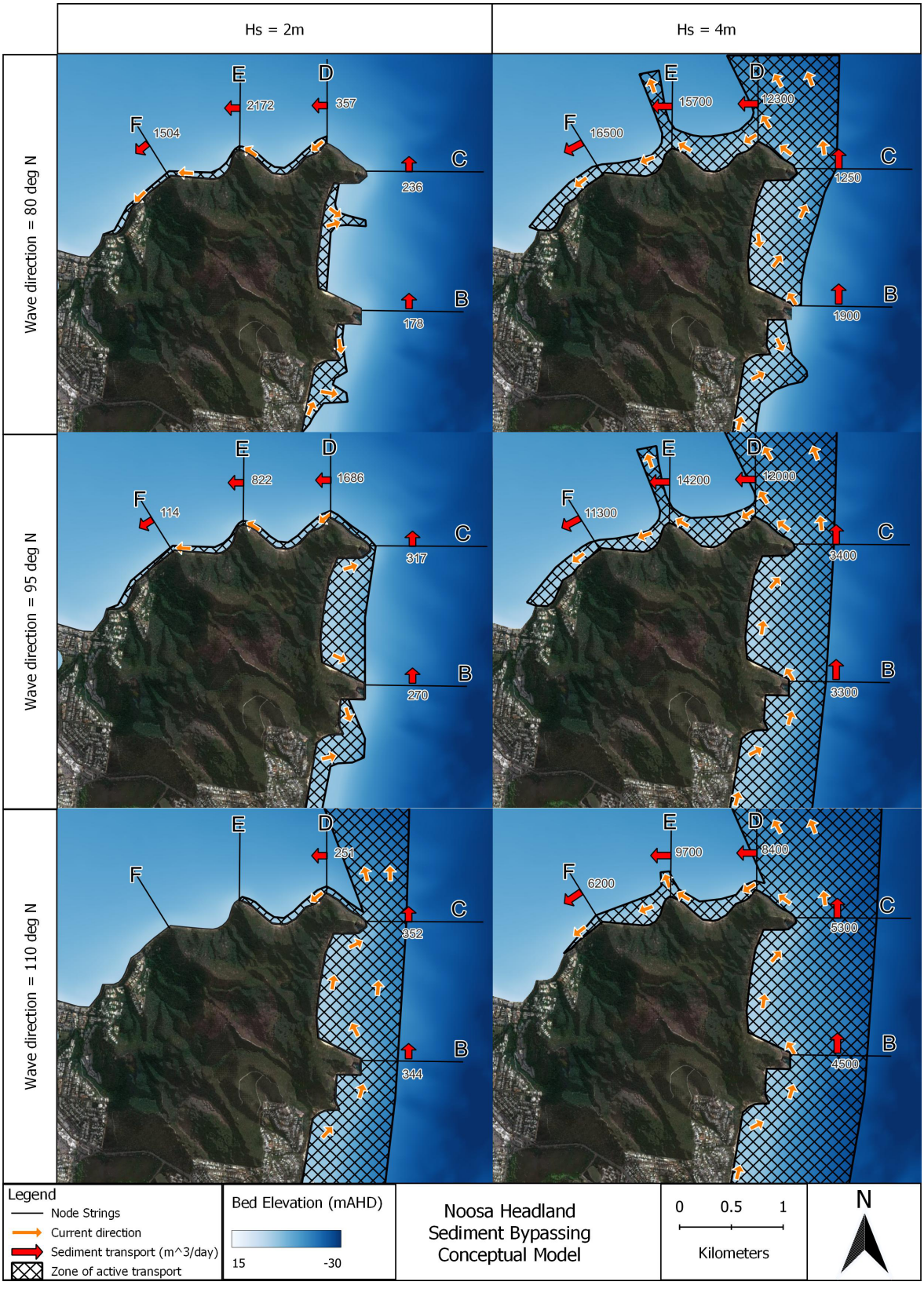


**Figure 12:** Noosa Headland sediment bypassing conceptual model.

The two pathways for sand migration around the headland are a nearshore attached pathway and a cross-embayment pathway. The nearshore attached pathway behaves as previously hypothesized, with wave breaking energizing the nearshore environment and continuously moving sediment around the headland. The cross-embayment pathway shows that sediment transport can become detached from the headland and migrate across the embayment to the north of the headland (Laguna Bay), a conclusion also found at other headlands (Goodwin et al., 2013). Of particular interest, this cross-embayment pathway was not only set up at the largest apex of the headland (Hell's Gate), where there is considerable updrift distance to energise a longshore current that can transport the sediment into this cross embayment, but also at Dolphin Point, a minor apex with less set-up distance for currents to form. The sediment that enters the cross-embayment pathway at Hell's Gate moves into water that is up to 20m deep, while sediment from Dolphin Point follows a pathway across an area where the seabed is between 10m and 12m, suggesting that this sediment may remain available as a sand source for the northern area of the headland under suitable conditions. Sediment moving through this cross-embayment pathway, from either headland apex, settles out in Laguna Bay as the currents dissipate, resulting in the seabed updrift of the headland being significantly thicker with nearshore sediments (Jones and Stephens, 1981) and much shallower than downdrift locations at a similar distance from the shoreline. As a result of continuous energizing by wave breaking, the nearshore attached pathway is the faster mode of transport from the headland apex to the downdrift beaches north of Noosa River.

The results of this study indicate that there are also two 'modes' of bypassing of the headland, with the previously hypothesized 'sand slug' mode occurring with sufficient wave forcing, generally considered to be when $H_s > 2.5$m, and a smaller magnitude 'trickle' bypassing occurring under smaller wave conditions ($1\text{m} > H_s < 2.5\text{m}$). This wave height threshold aligns with the regional definition of 'storm' conditions and 'modal' conditions that has a statistical boundary at $H_s = 2.1$m for summer wave and 1.75m for winter waves. Despite the 'storm' conditions providing significantly more energy to the nearshore environment, they only account for approximately 6% of days at the site, while the modal conditions that force the 'trickle' bypassing make up the vast majority of days at the site. The 'sand slug' mode that occurs under 'storm' conditions makes up approximately 60-70% of total bypassing by volume for the exposed headland apexes to the east of Noosa Headland, while the more protected headlands on the northern side of the headland show an increasing proportion of 'trickle' bypassing, due in large part, to the shallower sea bead at these apexes.

## 6.2 Influence of regional climate drivers

The relationship between regional climate conditions and sediment bypassing at each headland apex was directly measurable within this study, with ENSO phase, seasonality, storminess and synoptic modality all assessed. The most significant of these was seasonality, with summer periods producing 80% to 150% more bypassing than winter periods, with spring and autumn being transitional between these two. Summer wave conditions at the site are more northerly orientated and more energetic than winter conditions as the site is exposed to tropical storm and cyclone conditions in the Coral Sea, northeast of the site. During winter, the Coral and Tasman Seas are dominated by extra-tropical low-pressure systems in the Tasman Sea, that produce southerly wave conditions that the site is partially protected from due to offshore islands and the overall shoreline orientation. This is also seen in the synoptic modality, with summer modalities more significant to bypassing than winter modalities. For Hell's Gate, which is fully exposed to waves from all synoptic modes, easterly and southeasterly waves are the most significant, while for the apexes on the north of the headland, synoptic modes which produce easterly and northeasterly wave conditions are the most significant. The significance of storminess was discussed in the previous section, while ENSO phase was only significant for Hells Gate, which aligns with the previous conclusions from the site (Wishaw et al., 2021), due to ENSO phase modulating the modal wave power from southerly synoptic patterns(Mortlock and Goodwin, 2016).

## 6.3 Future climate implications

Predictions of future wave climate scenarios remain complicated due to the multitude of influencing factors and their complex interaction between each other. At the study site, the wave climate consists of a combination of storm and modal wave conditions from various sources that are all predicted to be influenced by a warming planet. Modal synoptic patterns in the Coral and Tasman Seas are expected to change their relative power in future, due to a southward migration of the sub-tropical ridge that controls the location of these patterns. This change in wave power is the result of the relative weakening of southerly wave forming synoptic modes and strengthening of the easterly wave forming synoptic modes (Mortlock and Goodwin, 2015). Storm waves, typically generated from tropical lows and cyclones in the Coral Sea are likely to change in future climate scenarios, with a poleward migration of

maximum cyclone intensity suggested, that would bring wave generation closer to the site (Kossin et al., 2014). Global forecasts of the average wave climate suggests both an increase in overall wave power (Reguero et al., 2019), and a shift in mean deep-water wave direction of between 5–15° by the end of the century (Morim et al., 2019). However, each of these findings are provided in the context of remaining uncertainty of global climate projections and the ability of models to suitably predict changes to such a degree of accuracy that deterministic forecasts of future wave climates can be derived. Nonetheless, with the tools developed in this research we can explore how different scenarios of wave climate modification may influence the study site. Predictions of weakening southerly modes of wave formation and strengthening easterly modes and north-east storm waves would migrate the average wave climate in anti-clockwise direction. This would have the effect of strengthening conditions that create sediment transport on the north side of the headland, while weakening conditions that drive transport on the east side. At present, the wave climate exists in a 'goldilocks' zone where transport volumes on the east and north sides of the headland are slightly skewed towards increased transport on the north side, resulting in net erosion of the beaches on the north side. Predicted changes would enhance this pattern, with increased erosive pressure on the northern beaches, with less sediment transport around the large headland apex at the east of the headland, resulting in increased sand starvation of these beaches.

## 7. Conclusions

This research developed a tool for accurately forecasting headland sediment transport in a highly efficient manner which was used to explore changes in sediment transport volume with respect to changes in wave conditions and regional climate drivers that control wave conditions. Our findings reveal that headland transport occurs in two different modes; a 'trickle' bypassing mode occurs under conditions with lower wave heights ($H_s$<2m) and the migration of large 'sand slugs' under larger wave heights. Despite their difference in transport rate, these two modes can provide similar annual transport volumes due to the greater prevalence of smaller wave conditions. Sediment being transported around the headland was found to follow two pathways; a more energetic headland attached pathway that remained in the shallower area around the headland and a cross-embayment pathway that became detached from the headland and transported sediment into the deep water north of the headland, where transport rates were significantly lower.

Headland sediment transport was sensitive to changes in both wave height and direction, with different conditions required for sediment transport on the east and north side of the headland. Balanced migration of sediment transport around the headland was reliant on the wave direction remaining between the current mean wave direction and one standard deviation south (15 degrees) of the existing mean wave direction. Seasonality was found to be the most significant climate influence on headland bypassing at the site, with synoptic modality significant for 'trickle' bypassing, where summer synoptic patterns that generated east and northeast waves produced the most bypassing. ENSO phase was only significant for the easterly orientated apexes, with La Niña conditions providing more bypassing than either El Niño or ENSO-neutral conditions, while the strength of this pattern was reduced for northerly orientated headland apexes.

Finally, the research considered the implications of changing wave conditions under a future climate scenario. While the precise magnitude of this change continues to be developed, this research considered the most likely scenario of an anticlockwise rotation of the wave environment. This change in the wave climate would reduce bypassing of the east face of the headland and increase the transport on the north side, resulting in more frequent sediment starvation of the protected beaches on the north side of the headland.

## 8. Acknowledgements

The authors are grateful for the support and contributions from the University of the Sunshine Coast and the support from BMT commercial. The authors also acknowledge the valuable contribution from the Queensland Government's Department of Environment and Science who have provided data for this research.

## 9. Open Research

The modelling input and synoptic clustering data used for the development of the process-based model and the synoptic clustering outputs in the study are available at the University of the Sunshine Coast Research Bank via https://doi.org/10.25907/00751 with open access.

## 10. References


Barnes, M., Cullen, J., O'Malley-Jones, K., 2019. Noosa Spit Shoreline Erosion Management Plan, BMT.

Barnes, M., Huxley, C., Andrews, M., 2013. Sunshine Coast Regional Council - Coastal processes study for the Sunshine Coast, BMT WBM Brisbane, Australia.

Barnes, M.T., Ian; Wood, Peter; Voisey, Chris, 2015. Assessment of Capital Works Options to Mitigate Shoaling at the Mooloolaba Harbour Entrance, Australasian Coast & Ports, Auckland, New Zealand.

Benedet, L., Dobrochinski, J.P.F., Walstra, D.J.R., Klein, A.H.F., Ranasinghe, R., 2016. A morphological modeling study to compare different methods of wave climate schematization and evaluate strategies to reduce erosion losses from a beach nourishment project. Coastal Engineering, 112, 69-86.

BMT Commercial Australia, 2022. TUFLOW 2D/3D Flexible Mesh Modelling.

Dabbura, I., 2018. K-means Clustering: Algorithm, Applications, Evaluation Methods, and Drawbacks.

Delft University of Technology, 2016. SWAN Scietific and Technical Documentation, version 41.10.

Deltares, 2022. X Beach.

Gaudet, J., Roy, A., Best, J., 1994. Effect of orientation and size of Helley-Smith sampler on its efficiency Journal of Hydraulic Engineering, 120(6), 758-766.

George, D.A., Largier, J.L., Storlazzi, C.D., Barnard, P.L., 2015. Classification of rocky headlands in California with relevance to littoral cell boundary delineation. Marine Geology, 369, 137-152.

Geoscience Australia, 2017. High-resolution depth model for the Great Barrier Reef – 30m.

Goodwin, I.D., Freeman, R., Blackmore, K., 2013. An insight into headland sand bypassing and wave climate variability from shoreface bathymetric change at Byron Bay, New South Wales, Australia. Marine Geology, 341, 29-45.

Goodwin, I.D., Mortlock, T.R., Browning, S., 2016. Tropical and extratropical-origin storm wave types and their influence on the East Australian longshore sand transport system under a changing climate. Journal of Geophysical Research: Oceans, 121(7), 4833-4853.

Harris, P.T., Heap, A.D., Bryce, S.M., Porter-Smith, R., Ryan, D.A., Heggie, D.T., 2002. Classification of Australian Clastic Coastal Depositional Environments Based Upon a Quantitative Analysis of Wave, Tidal, and River Power. Journal of Sedimentary Research, 72(6), 858-870.

Helley, E.J., Smith, W., 1971. Development and Calibration of a Pressure-Difference Bedload Sampler. U.S Geological Survey.

Jones, M.R., Stephens, A.W., 1981. Sand transport at Noosa. Queensland: Summary, Geological Survey of Queensland

King, E.V., Conley, D.C., Masselink, G., Leonardi, N., McCarroll, R.J., Scott, T., Valiente, N.G., 2021. Wave, Tide and Topographical Controls on Headland Sand Bypassing. Journal of Geophysical Research: Oceans, 126(8).

Klein, A.H.F., Vieira da Silva, G., Taborda, R., da Silva, A.P., Short, A.D., 2020. Headland Bypassing and Overpassing: form, processes and applications, Sandy Beach Morphodynamics. Elsevier, pp. 814.

Kossin, J.P., Emanuel, K.A., Vecchi, G.A., 2014. The poleward migration of the location of tropical cyclone maximum intensity. Nature, 509(7500), 349-352.

Marine Geophysics Laboratory, 2022. Current Meter: Marotte HS.

McCarroll, R.J., Masselink, G., Valiente, N.G., King, E.V., Scott, T., Stokes, C., Wiggins, M., 2021. An XBeach derived parametric expression for headland bypassing. Coastal Engineering, 165.

Morim, J., Hemer, M., Wang, X.L., Cartwright, N., Trenham, C., Semedo, A., Young, I., Bricheno, L., Camus, P., Casas-Prat, M., Erikson, L., Mentaschi, L., Mori, N., Shimura, T., Timmermans, B., Aarnes, O., Breivik, Ø., Behrens, A., Dobrynin, M., Menendez, M., Staneva, J., Wehner, M., Wolf, J., Kamranzad, B., Webb,

A., Stopa, J., Andutta, F., 2019. Robustness and uncertainties in global multivariate wind-wave climate projections. Nature Climate Change(9), 711–718.
Mortlock, T.R., Goodwin, I.D., 2015. Directional wave climate and power variability along the Southeast Australian shelf. Continental Shelf Research, 98, 36-53.
Mortlock, T.R., Goodwin, I.D., 2016. Impacts of enhanced central Pacific ENSO on wave climate and headland-bay beach morphology. Continental Shelf Research, 120, 14-25.
NOAA, 2022. Daily Mean Composites.
Paula da Silva, A., Vieira da Silva, G., Perez, J., 2021. Wave Generation Zones off the East Australian Coast, Australiasian Coasts and Ports 2021, Christchurch, New Zealand.
Queensland Government, 2012. Queensland coastal risk and bathymetric LiDAR: a pilot study for collecting near-shore bathymetry, Queensland Department of Science, Information Technology, Innovation and the Arts, Brisbane, Australia.
Queensland Government, 2019a. Tide Monitoring Sites.
Queensland Government, 2019b. Wave Monitoring Sites.
Reguero, B.G., Losada, I.J., Mendez, F.J., 2019. A recent increase in global wave power as a consequence of oceanic warming. Nat Commun, 10(1), 205.
Saha, S., Shrinivas Moorthi, Xingren Wu, Jiande Wang, Sudhir Nadiga, Patrick Tripp, David Behringer, Yu-Tai Hou, Hui-ya Chuang, Mark Iredell, Michael Ek, Jesse Meng, Rongqian Yang, Malaquías Peña Mendez, Huug Van Den Dool, Qin Zhang, Wanqiu Wang, Mingyue Chen, Emily Becker., 2014. The NCEP Climate Forecast System Version 2. Journal of Climate, 27(6), 2185-2208.
Saha, S.N., C. Thiaw, J. Wang, W. Wang, Q. Zhang, H. M. Van Den Dool, H.-L. Pan, S. Moorthi, D. Behringer, D. Stokes, M. Peña, S. Lord, G. White, W. Ebisuzaki, P. Peng, P. Xie, 2006. The NCEP Climate Forecast System Journal of Climate, 19(15).
Silva, A.P.D., Vieira da Silva, G., Strauss, D., Murray, T., Woortmann, L.G., Taber, J., Cartwright, N., Tomlinson, R., 2021. Headland bypassing timescales: Processes and driving forces. Sci Total Environ, 793, 148591.
Splinter, K.D., Coco, G., 2021. Challenges and Opportunities in Coastal Shoreline Prediction. Frontiers in Marine Science, 8.
Splinter, K.D., Davidson, M.A., Golshani, A., Tomlinson, R., 2012. Climate controls on longshore sediment transport. Continental Shelf Research, 48, 146-156.
Van Rijn, L.C., 2007a. United view of sediment transport by currents and waves I: Initiation of motion, Bed roughness and bed load transport. Journal of Hydraulic Engineering, 133(6), 649-667.
Van Rijn, L.C., 2007b. United view of sediment transport by currents and waves II: Suspended transport. Journal of Hydraulic Engineering, 133(6), 668-689.
Van Rijn, L.C., 2007c. United view of sediment transport by currents and waves III: Graded beds. Journal of Hydraulic Engineering, 133(6), 761-775.
Vieira da Silva, G., Stauss, D., Murray, T., Tomlinson, R., Paula da Silva, A., 2021. Impacts of Climate Change on Sediment Transport Rates Around Burleigh Heads, Australasian Coasts & Ports 2021 Conference, Christchurch.
Vieira da Silva, G., Toldo, E.E., Klein, A.H.d.F., Short, A.D., Woodroffe, C.D., 2016. Headland sand bypassing — Quantification of net sediment transport in embayed beaches, Santa Catarina Island North Shore, Southern Brazil. Marine Geology, 379, 13-27.
Vieira da Silva, G., Toldo Jr, E.E., Klein, A.H.d.F., Short, A.D., 2018. The influence of wave-, wind- and tide-forced currents on headland sand bypassing – Study case: Santa Catarina Island north shore, Brazil. Geomorphology, 312, 1-11.
Wishaw, D., Leon, J., Fairweather, H., Crampton, A., 2021. Influence of wave direction sequencing and regional climate drivers on sediment headland bypassing. Geomorphology, 383.
Wishaw, D., Leon, J.X., Barnes, M., Fairweather, H., 2020. Tropical Cyclone Impacts on Headland Protected Bay. Geosciences, 10(5).

# Appendix 1 Model Configuration

Table 3: SWAN model calibration parameters

| Parameter | Value |
|---|---|
| Model mode | Gen 3 |
| Friction expression | Collins (1972) |

| | |
|---|---|
| Collins bottom friction coefficient | 0.015 |
| Numerics | BSBT |
| dabs | 0.02 |
| drel | 0.02 |
| curvant | 0.02 |
| npnts | 98.0 |
| Non-stationary computation | On |
| mxitns | 15 |
| limiter | 0.1 |
| DIRIMPL | On |
| cdd | 0.5 |
| Timestep | 1.0 hours |

661 Table 4: TUFLOW model calibration parameters

| Parameter | Value |
|---|---|
| momentum mixing model | Smagorinsky |
| horizontal gradient limiter | LCD |
| bottom drag model | ks |
| Reference salinity | 35.0 |
| Reference temperature | 20.0 |
| Reference mslp | 1011 |
| Reference density | 1025 |
| Density air | 1.18 |
| Kinematic viscosity | 1.0e-6 |
| global horizontal eddy viscosity | 0.2 |
| global vertical eddy viscosity limits | 1.0e-4, 9999.0 |
| bottom roughness | 0.05 |
| waves | On |
| Output interval | 0.25 hours |

662